NUCL SCI TECH (2017) 28:136
DOI 10.1007/s41365-017-0279-7

Study of relation between the gamma flux buildup factors and source geometry by M-C simulation

Ali Rasouli[1] · **Hossein Tavakoli-Anbaran**[1]

Received: 30 September 2016 / Revised: 16 November 2016 / Accepted: 13 December 2016 / Published online: 21 August 2017

Abstract This paper is to achieve a gamma-ray source with the lowest rate of buildup factor, which is of great importance in medical, industrial and agricultural sciences. The flux buildup factor of gamma rays is calculated by the MCNP code for point, linear, surface and volume sources with shield layers of lead, iron and aluminum. The results show that for the high Z shielding material, the flux buildup factor of coaxial cylindrical sources is the lowest (1.6–2.3) of all sources, while for low Z shielding materials, the coaxial disk surface sources have smaller buildup factor (1.45–1.6).

Keywords Gamma flux buildup factor · Monte Carlo method · ^{137}Cs · ^{60}Co and ^{16}N gamma sources

1 Introduction

Nowadays nuclear technology is used in the industry, agriculture and medicine. Therefore, protection against harmful effects of external radiations is regarded significant. Due to high penetration of gamma ray and its widespread application in radiotherapy, shielding of gamma radiation is important. Radiotherapy is used to treat almost every type of solid tumor [1–5]. The degree of tissue damage depends not only on quantity of radiation but also individual susceptibility of each organ to radiation damage. Parts of the body are shielded against radiation. For example, in radiotherapy of breast tumor, the nearby healthy tissue is shielded with a cap [2]; and in maxillafacial tumor radiotherapy, poly cyclohexane is used to avoid gamma-rays irradiation of healthy tissues surrounding the tumors [6]. In fact, shields are always present for protection of healthy tissue.

However, shields can cause multiple scattering of photons, and some of the gamma rays are inclined toward healthy tissues. The flux received by healthy tissues must be accurately calculated. Using shields to prevent radiation from reaching to healthy tissues is conventional procedure in radiography. For instance, shielding is used to protect the genitalia during pelvis and lower parts radiographic examinations [7]. Besides, shields of high atomic number materials are used in CT scans, such as the lead shields in head and neck CT scan to protect the surface tissue [8].

The presence of shielding material along with radiations is described by the buildup factor. It is associated with multiple scattering of X- and gamma rays within the shields. Buildup factor leads to accumulation of additional flux in specific areas (e.g., the healthy tissue). According to its importance in medical [9, 10], industrial [11–13], agriculture [14] and nuclear areas [15–18], buildup factors have been measured, but precise determination of the coefficients in all materials through experiment is not easy. So, the coefficients are often calculated by using photon absorption and scattering cross sections. The codes to calculate buildup factors include BIGGI-4T, EGS4, PALLAS-PL and Monte Carlo N-particle (MCNP).

In early 1900s, the calculation of buildup factor for different elements was the goal of most studies. In 1993, Harima studied the relationship between flux buildup factor with energy and material compositions [19]. Other groups

✉ Hossein Tavakoli-Anbaran
tavakoli-anbaran@shahroodut.ac.ir;
tavakoli.Anbaran@gmail.com

[1] Faculty of Physics, Shahrood University of Technology, Shahrood, Iran

studied parameters associated with buildup factor in recent decades [10–17] by using MCNP and the other codes. In this study, we investigated the effect of source geometry on flux buildup factor by Monte Carlo method.

1.1 Method of calculation

At first, using the MCNP code, the flux buildup factor was calculated for ^{60}Co gamma rays of 1.17 and 1.33 MeV, and their average energy of 1.25 MeV, in different geometries, with a lead shielded detector. Then, three materials of different atomic numbers were used for comparison, at 1.17 and 1.33 MeV. The atomic numbers, aluminum ($Z = 13$), iron ($Z = 26$) and lead ($Z = 82$), were selected so that the changes of buildup factor with atomic number could be studied.

Geometries of photon sources used in the simulations were: (1) isotropic point sources; (2) isotropic linear sources in X, Y and Z axis; and (3) plate and disk isotropic superficial sources of cylindrical, spherical and cubic isotropic volumetric sources.

Figure 1 shows schematically the source-shield-detector geometries. The shield thickness was 1.55 cm, and the sources were centered at (0, 1.27, 0).

Simulations were performed using two isotropic and parallel beam models, with the tally of F4, which outputs the photon numbers per unit volume of the detector. The results are shown in Fig. 2. In the following, changes of buildup factor at 1.17 and 1.33 MeV for lead, iron and aluminum will be examinated.

Flux buildup factor changing with energy and shielding materials was simulated, and sources with the lowest buildup factor were determined. The buildup factors at 0.66, 1.25 and 6.20 MeV for the 12 source geometries are shown in Fig. 3. In Fig. 4, the buildup factors of the three shielding materials at the same energy are compared.

2 Results

From Figs. 2, 3 and 4, the flux buildup factor depends on the source geometric shapes, γ-ray energy and atomic number of the shield. Among the photon interactions with shielding materials (photoelectric, Compton and pair production), Compton scattering is dominant effect. Occurrence probabilities of the total photon interactions and the Compton interaction are shown in Fig. 5, from which photon cross sections for Al, Fe and Pb can be obtained, using the Xcom Gamma Cross Section database [20].

In Fig. 5b, in the energy range of interest (0.66–6.20 MeV), the Compton scattering probability for Pb differs greatly from those for Al and Fe. The Compton scattering probabilities for Al and Fe decrease with increasing energy, while the Compton scattering probability for Pb increases with energy. So, the Pb buildup factor changes differently from those of Al and Fe (Fig. 3). Escape probability of scattered energetic photons through the Pb shield is greater than that of low-energy photons. For the Al and Fe shields, Compton interactions of ^{137}Cs γ-rays produce more secondary photons than ^{60}Co and ^{16}N, hence the greater buildup factor of ^{137}Cs in Fig. 3.

For ^{60}Co source, the flux buildup factor of Fe shields is greater than those of Pb and Al. The reason lies in the total interaction probability of photons for these elements. The photon absorption probability increased with scattering interaction in the lead shield, so less scattered photon flux is recorded in the detector than ferrous shield. In parallel beams, decreased buildup factor is related to small surface of the shield that photon scattering interaction is involved.

For Pb, coaxial cylindrical sources with shield and detector have the least buildup factor of all the sources (Fig. 3). After interaction inside the volume source, less energy photons are produced in the shield, which has high absorption probability. The coaxial cylindrical source with

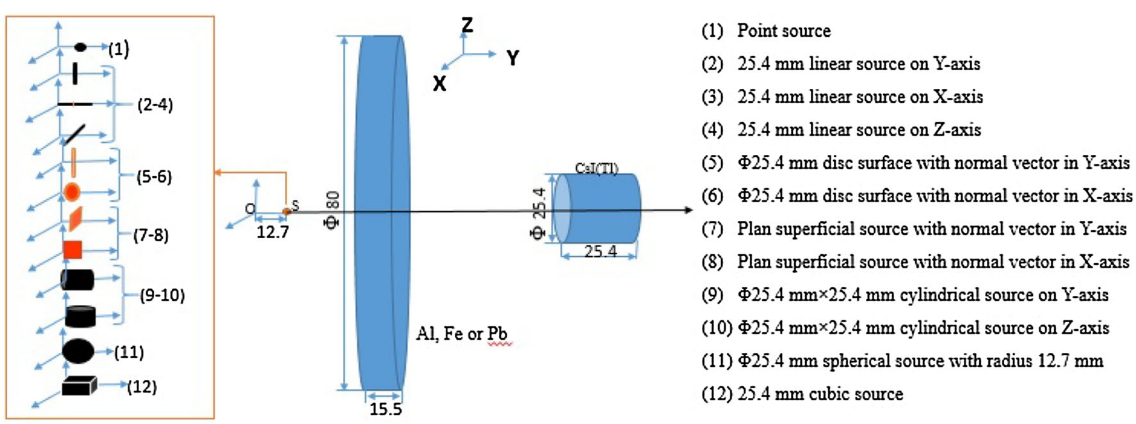

Fig. 1 (Color online) Schematics of the source-shield-detector system (in mm)

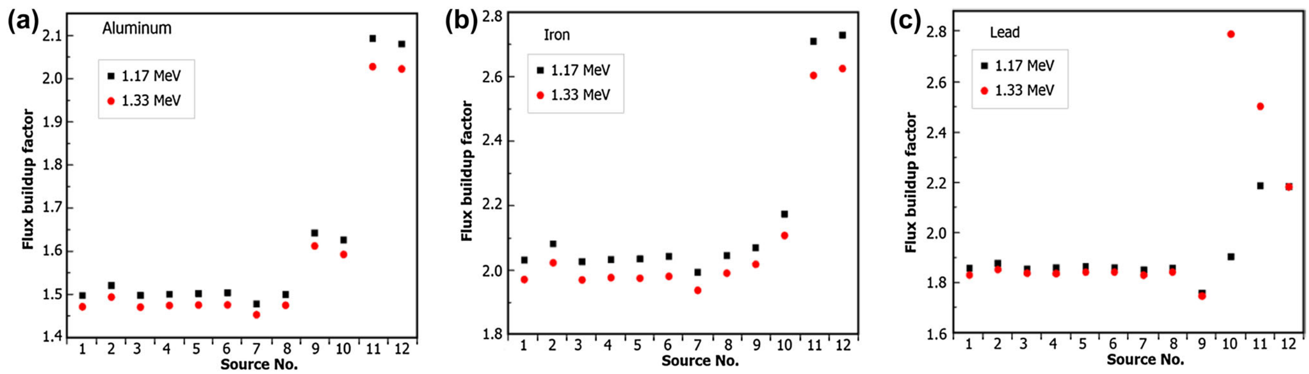

Fig. 2 (Color online) Simulated c-ray flux buildup factors for the 12 source geometries at 1.17 and 1.33 MeV with (**a**) Al, (**b**) Fe and (**c**) Pb shields of 1.55 cm thickness

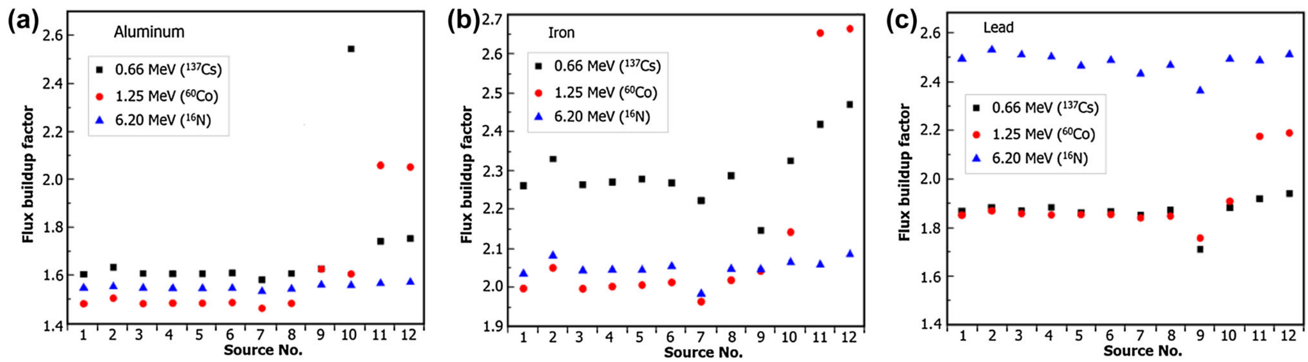

Fig. 3 (Color online) Simulated c-ray flux buildup factors for the 12 source geometries at 0.66, 1.25 and 6.20 MeV with (**a**) Al, (**b**) Fe and (**c**) Pb shields of 1.55 cm thickness

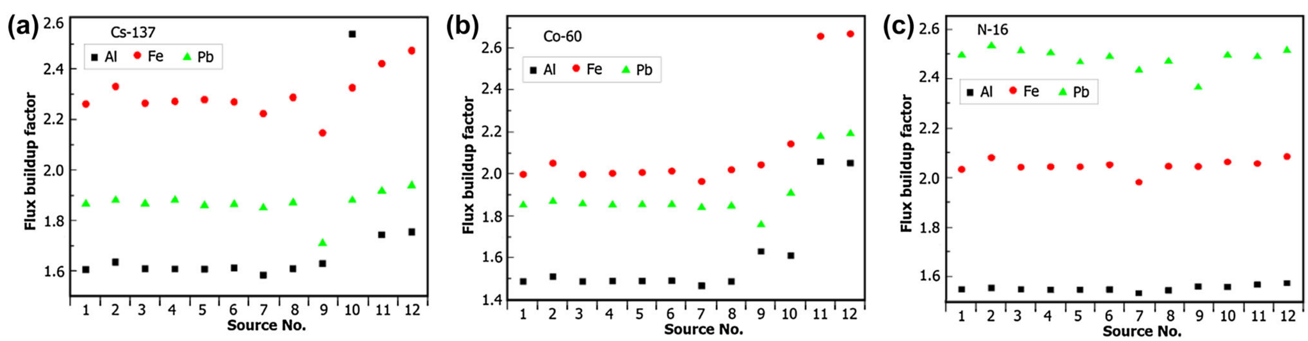

Fig. 4 (Color online) Comparison of the flux buildup factors regarding to the source types for Al, Fe and Pb at (**a**) Cs-137, (**b**) Co-60 and (**c**) N-16. Repetition

Fig. 5 (Color online) Mass attenuation coefficient changes according to energy for (**b**) Compton and (**a**) total interactions in energy range 1 keV to 100 MeV

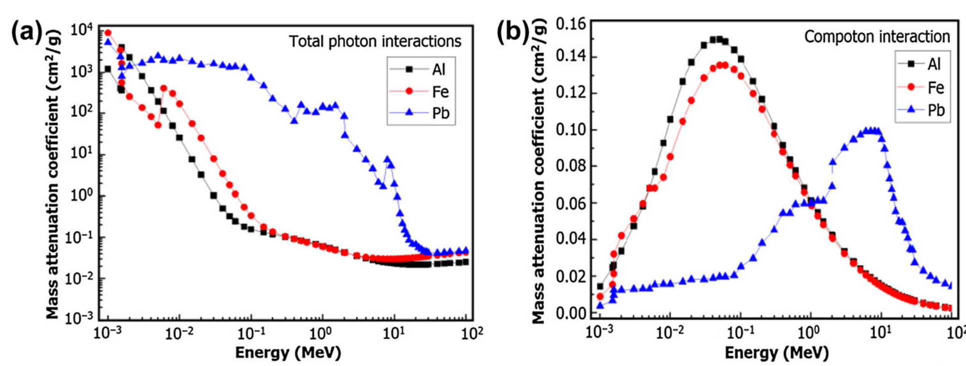

Table 1 Simulation results for aluminum, iron and lead shields to the three kinds of sources in the 12 geometries

No. of source geometry			1	2	3	4	5	6	7	8	9	10	11	12
^{137}Cs (0.66 MeV)	Al	B	1.605	1.635	1.610	1.608	1.608	1.611	1.583	1.609	1.630	2.540	1.740	1.750
		σ_B/B	0.005	0.006	0.006	0.006	0.006	0.006	0.007	0.006	0.005	0.007	0.006	0.007
	Fe	B	2.262	2.332	2.264	2.271	2.279	2.269	2.223	2.288	2.147	2.326	2.422	2.473
		σ_B/B	0.007	0.008	0.008	0.008	0.008	0.008	0.010	0.008	0.007	0.009	0.009	0.009
	Pb	B	1.866	1.882	1.868	1.882	1.860	1.865	1.851	1.872	1.709	1.881	1.918	1.939
		σ_B/B	0.012	0.013	0.013	0.013	0.013	0.013	0.016	0.014	0.010	0.014	0.014	0.015
^{60}Co (1.25 MeV)	Al	B	1.484	1.507	1.484	1.486	1.486	1.488	1.465	1.485	1.628	1.607	2.057	2.050
		σ_B/B	0.005	0.006	0.006	0.006	0.006	0.006	0.007	0.006	0.006	0.007	0.008	0.009
	Fe	B	1.997	2.050	1.996	2.000	2.000	2.013	1.963	2.018	2.042	2.142	2.657	2.668
		σ_B/B	0.007	0.007	0.007	0.007	0.007	0.007	0.009	0.008	0.007	0.009	0.010	0.010
	Pb	B	1.850	1.868	1.856	1.851	1.853	1.853	1.839	1.846	1.756	1.907	2.177	2.191
		σ_B/B	0.008	0.009	0.009	0.009	0.009	0.009	0.010	0.010	0.008	0.010	0.012	0.013
^{60}Co (1.17 MeV)	Al	B	1.497	1.520	1.497	1.500	1.501	1.503	1.477	1.499	1.642	1.626	2.093	2.080
		σ_B/B	0.005	0.006	0.006	0.006	0.005	0.006	0.007	0.006	0.006	0.007	0.008	0.008
	Fe	B	2.031	2.081	2.027	2.033	2.035	2.043	1.993	2.046	2.070	2.174	2.700	2.729
		σ_B/B	0.006	0.007	0.007	0.007	0.007	0.007	0.009	0.008	0.007	0.008	0.010	0.010
	Pb	B	1.860	1.879	1.857	1.862	1.866	1.862	1.853	1.860	1.760	1.900	2.180	2.185
		σ_B/B	0.009	0.009	0.009	0.009	0.010	0.010	0.010	0.010	0.009	0.011	0.013	0.013
^{60}Co (1.33 MeV)	Al	B	1.493	1.470	1.474	1.475	1.475	1.452	1.474	1.612	1.592	2.027	2.022	1.471
		σ_B/B	0.005	0.005	0.005	0.005	0.005	0.006	0.007	0.006	0.006	0.007	0.008	0.008
	Fe	B	1.971	2.023	1.970	1.977	1.975	1.981	1.937	1.991	2.018	2.107	2.603	2.625
		σ_B/B	0.006	0.007	0.007	0.007	0.007	0.007	0.008	0.007	0.007	0.008	0.009	0.010
	Pb	B	1.833	1.854	1.840	1.839	1.844	1.844	1.832	1.844	1.749	2.790	2.502	2.184
		σ_B/B	0.008	0.009	0.009	0.009	0.009	0.009	0.010	0.009	0.008	0.011	0.012	0.013
^{16}N (6.2 MeV)	Al	B	1.549	1.555	1.549	1.548	1.548	1.548	1.535	1.545	1.562	1.560	1.568	1.573
		σ_B/B	0.005	0.005	0.005	0.005	0.005	0.005	0.006	0.006	0.005	0.005	0.005	0.006
	Fe	B	2.035	2.081	2.043	2.045	2.045	2.054	1.983	2.047	2.046	2.064	2.058	2.085
		σ_B/B	0.006	0.007	0.007	0.007	0.007	0.007	0.008	0.007	0.006	0.007	0.006	0.007
	Pb	B	2.496	2.533	2.513	2.505	2.467	2.490	2.434	2.471	2.365	2.495	2.489	2.515
		σ_B/B	0.010	0.010	0.010	0.010	0.010	0.010	0.011	0.010	0.010	0.011	0.010	0.011

shield has the less solid angle than other directions, which affects the buildup factor. For shields of intermediate atomic number, coaxial disk source with shield has the lowest buildup factor, the total flux is the lowest of all the sources, but the non-contact flux is greater than the other sources. In this situation, coaxial disk and plate sources have the best performance in terms of the buildup factor.

At the energies over 6 MeV, the pair production interactions in high atomic number materials can occur and the annihilated photons may reach the detector, and flux buildup factor of Pb is greater than those of Al and Fe.

The error of the results in the Monte Carlo method is a relative quantity in the simulation outputs and is of utmost importance; therefore, we will dedicate this section of our study to this quantity. According to the definition of the buildup factor which is “the ratio of the value of a specific radiation quantity at each point to the uncollided component of that quantity,” the relative error of the flux buildup factor, σ_B/B, is calculated by $\sigma_B/B = [(\sigma_{\varphi\_\mathrm{uncollided}}/\varphi_{\mathrm{uncollided}})^2 + (\sigma_T/\varphi_T)^2]^{1/2}$, where $\sigma_{\varphi\_\mathrm{uncollided}}/\varphi_{\mathrm{uncollided}}$ is the relative error of the uncollided flux, and σ_T/φ_T is the relative error of the total flux.

For the 12 source geometries, from Table 1, the relative error for aluminum shielding to ^{137}Cs, ^{60}Co and ^{16}N sources is of the order of one thousandth; the maximum relative error for iron shielding to ^{60}Co source is of the order of one hundredth, and of the order of one thousandth to ^{137}Cs and ^{16}N sources; and the maximum relative error is of the order of one hundredth for lead shielding to all the sources. According to the standards of the Monte Carlo method in simulations, all the errors have reasonable values and the calculations have adequate validity.

3 Conclusion

Flux buildup factors of ^{137}Cs, ^{60}Co and ^{16}N γ-rays in shielding materials of Al, Fe and Pb are calculated by Monte Carlo method for linear, surface and volume sources types in different axial directions. Secondary photons are the effective factor on buildup factor. The sources cover energy range of 0.66–6.20 MeV, while the 1.17 and 1.33 MeV γ-rays of ^{60}Co, and the average energy (1.25 MeV), are used.

According to simulation results, among the point, linear, surface and volume sources along X, Y and Z axis, the coaxial volumetric cylindrical source-shield-detector system has the least flux buildup factor. For low atomic number materials, coaxial disk surface source-shield-detector systems have small flux buildup factor. Then simulation errors are in the order of thousandths.

References

1. F. Eichmiller, Device and method for shielding healthy tissue during radiation therapy. US Patent. 5,190,990(1993)
2. J.S. Vaidya, J.S. Tobias, M. Baum et al., Intraoperative radiotherapy for breast cancer. Lancet Oncol. **5**, 165–173 (2004). doi:10.1002/ijc.21727
3. W. Yang, Y. Kim, X. Wu et al., Rotating-shield brachytherapy for cervical cancer. Phys. Med. Biol. **58**(11), 3931–3941 (2013). doi:10.1088/0031-9155/58/11/3931
4. A. Bezjak, R.B. Rumble, G. Rodriques et al., Intensity-modulated radiotherapy in the treatment of lung cancer. Clin. Oncol. (R CollRadiol). **24**, 508–520 (2012). doi:10.1016/j.clon.2012.05.007
5. J.L. Thalhofer, H.S. Roque, W.F. Rebello et al., Effect of external shielding for neutrons during radiotherapy for prostate cancer, considering the 2300CD linear accelerator and voxel phantom. Radiat. Phys. Chem. **95**, 267–270 (2014). doi:10.1016/j.radphyschem.2013.02.013
6. M. Farahani, F. Eichmiller, Metalpolysiloxane shields for radiation therapy of maxilla-facial tumors. Med. Phys. **18**, 273–278 (1991). doi:10.1118/1.596724
7. Sl Fawcett, S.J. Barter, The use of gonad shielding in pediatric hip and pelvis radiographs. Br. J. Radiol. **82**, 363–370 (2009). doi:10.1259/bjr/86609718
8. J.E. Nqaile, C.B. Uiso, P. Msaki et al., Use of lead shields for radiation protection of superficial organs in patients undergoing head CT examinations. Radiat. Prot. Dosim. **130**, 490–498 (2008). doi:10.1093/rpd/ncn095
9. D. Sardari, Estimation of gamma and x-ray photons buildup factor in soft tissue with Monte Carlo method. Appl. Radiat. Isot. **67**, 1438–1440 (2009). doi:10.1016/j.apradiso.2009.02.033
10. S. Manohara, Energy absorption buildup factor of human organs and tissues at energies and penetration depths relevant for radiotherapy and diagnostics. J. Appl. Clin. Med. Phys. **12**, 296–312 (2011). doi:10.1120/jacmp.v12i4.3557
11. S. Tejbir, K. Kumar, Chemical composition dependence of exposure buildup factor for some polymers. Ann. Nucl. Energy **36**, 114–120 (2009). doi:10.1016/j.anucene.2008.09.013
12. V. Singh, N. Badiger, Photon energy absorption buildup factors of gaseous mixtures used in radiation detector. Radioprotection **48**, 63–78 (2013). doi:10.1051/radiopro/2012024
13. S. Vishwanath, Gamma ray and neutron shielding properties of some alloy material. Ann. Nucl. Energy **64**, 301–310 (2014). doi:10.1016/j.anucene.2013.10.003
14. P. Vishal, Energy absorption buildup factor studies in some solids. IOSR J. Appl. Phys. **3**, 18–24 (2013). doi:10.1155/2014/359754
15. M.F. Chen, R.E. Faw, Buildup factors for gamma rays obliquely incident on slab shields of concrete, iron and lead. Radiation Protection Dosimetry. **51**: 27–33 (1994). http://rpd.oxfordjournals.org/content/51/1/27
16. A. Shirani, Calculation of exposure buildup factors for point isotropic gamma ray sources in stratified spherical shields of water surrounded by lead and optimization of water-lead combination. Iran. J. Sci. Technol. **1**: 29–34 (2013). http://www.shirazu.ac.ir/en
17. P. Priyada, An improved Compton scattering method for determination of concentration of solutions. Appl. Radiat. Isot. **70**, 2421–2427 (2012). doi:10.1016/j.apradiso.2012.06.026
18. M. Alamatsaz, A study of gamma ray exposure buildup factors in stratified shields for point isotropic sources, including the effects of incoherent scattering. J. Sci. Islam. Repub. Iran. **13**: 271–79 (2002). https://journals.ut.ac.ir/article_31724.html
19. Y. Harima, An historical review and current status of buildup factors calculation and application. Res. Lab. Nucl. React. Tokyo Inst. Technol. **41**, 631–672 (1993). doi:10.1016/0969-806X(93)90317-N
20. http://www.nist.gov/pml/data/xray_gammaray.cfm